Laser and Particle Beams

cambridge.org/lpb

Proton–boron fusion in a hydrogen-doped-boron target

Zhi Li[1,2], Zhao Wang[3], Guanchao Zhao[1,2], Bing Liu[1,2], Huasheng Xie[1,2], Muzhi Tan[1,2], Hairong Huang[1,2], Minsheng Liu[1,2], Dieter H. H. Hoffmann[1,2,4], Rui Cheng[3] and Di Luo[1,2]

[1]Hebei Key Laboratory of Compact Fusion, Langfang, China; [2]ENN Science and Technology Development Co., Ltd., Langfang, China; [3]Institute of Modern Physics, Chinese Academy of Sciences, Lanzhou, China and [4]School of Physics, Xi'An Jiaotong University, Xi'An, China

Research Article

Cite this article: Li Z *et al*. (2024) Proton–boron fusion in a hydrogen-doped-boron target. *Laser and Particle Beams* **42**, e5, 1–8. https://doi.org/10.1017/lpb.2024.2

Received: 21 November 2023
Revised: 30 March 2024
Accepted: 11 April 2024

Keywords:
hydrogen-doped-boron target; proton–boron fusion; α particle yield

Corresponding authors: Di Luo;
Email: luodia@enn.cn

Abstract

The proton–boron $^{11}\mathrm{B}\,(p,\alpha)\,2\alpha$ reaction (p-^{11}B) is an interesting alternative to the D-T reaction $\mathrm{D}\,(\mathrm{T},\mathrm{n})\,\alpha$ for fusion energy, since the primary reaction channel is aneutronic and all reaction partners are stable isotopes. We measured the α production yield using protons in the 120–260 keV energy range impinging onto a hydrogen–boron-mixed target, and for the first time present experimental evidence of an increase of α-particle yield relative to a pure boron target. The measured enhancement factor is approximately 30%. The experiment results indicate a higher reactivity, and that may lower the condition for p-^{11}B fusion ignition.

1. Introduction

The main development path for fusion energy is based on the deuterium–tritium (D-T) reaction. This may seem as an obvious choice, since this process provides the highest cross section at the lowest ignition temperature for all known fusion reactions. Recent progress in inertial fusion and magnetic confinement experiments underpin this trend (Refs 1–5). However, the feasibility within the present technical level should not be taken as granted but should be taken with a grain of salt. The start-up process for the ITER reactor will consume the available world amount of tritium and the resupply of tritium by lithium-n reactions on a scale that is necessary for a power reactor is a yet unsolved technological problem. Moreover, the D-T reaction provides most of the energy release in the form of high energy neutrons, which may pose an acceptance problem for the general public at least in some countries. Even though that all these problems will eventually find an acceptable solution, the fusion community has to keep an open mind for alternative fusion reactions (Refs 6–8). Currently, the p-^{11}B reaction with the generation of short-range high-linear energy transfer α particles is recently regarded as a novel promising approach for cancer treatment, i.e., proton–boron fusion therapy (Refs 9–11).

Early in the 20th century (1933), Oliphant and Rutherford (Ref. 12) pointed out the p-^{11}B fusion reaction channel, with an energy release of 8.7 MeV per reaction (Eq. 1). The prevailing belief is that the main reaction path is sequential. As shown in Fig. 1, the process involves the fusion of a proton and a boron nucleus to form an excited state of ^{12}C*, which then decays into an α particle (α_1) and an excited state of ^{8}Be*. Ultimately, three α particles can be obtained. The intermediate state could be a ground state ^{8}Be, alternatively, and the associated α (α_0) would have maximum energy. Additionally, there is a small fraction of ^{12}C* that directly decays into three α particles with equal energy, known as the direct channel:

$$p + {}^{11}\mathrm{B} \rightarrow 3\alpha + 8.7\ \mathrm{MeV}. \tag{1}$$

Becker et al. re-studied the p-^{11}B reaction cross section (Ref. 13) and analysed the reaction process in 1987, to be a sequential decay starting with an α emission from excited ^{12}C to ^{8}Be, and from there decaying into a pair of two α particles. More recently, Nevins and Swain (Ref. 14) developed the theoretical model in the energy range from $E_{c.\,m.} = 22$ keV to 3.5 MeV. Munch et al. (Ref. 15) summarized the tabulated data available via EXFOR (Ref. 16) for α_0 channel and compared them to their measurement. While most of the studies focus on the MeV energy range, there is a lack of data in the energy regime close to the first resonance (at around 160 keV). However, the p-^{11}B cross section in this energy region is critical for the ignition of a magnetic confinement thermonuclear fusion, as Putvinski et al. (Ref. 17) presented. Recently, an experiment on the large helical device has firstly measured p-^{11}B reactions in a magnetic

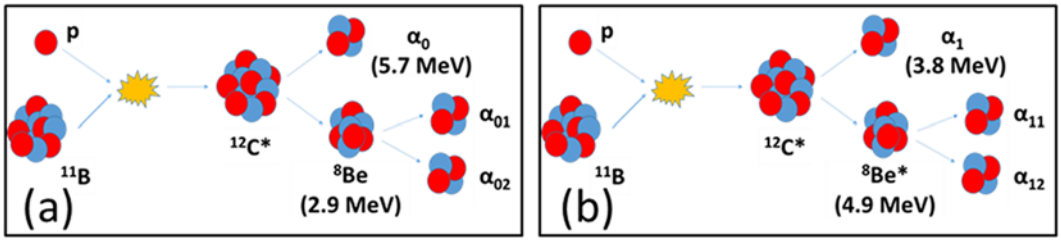

Figure 1. The schematic diagram of p-^{11}B sequential processes. A proton and a ^{11}B nuclei fuses into a ^{12}C* in excited state, then the ^{12}C* becomes (a) ^{8}Be in ground state by releasing α_0 or (b) ^{8}Be* in excited state by releasing $Pu^{239} + Am^{241} + Cm^{244}$. Finally, the ^{8}Be breaks up into two α particles.

confinement device, by injecting a neutral beam of protons at 160 keV (Ref. 18), which rises an interest of p-^{11}B studies in low energy. Thus, we decided to address this energy regime.

With the widespread emerging of high-power lasers in many laboratories worldwide stimulated by the chirped-pulse amplification technique, a series of laser-triggered p-^{11}B fusion experiments were performed and reported orders of magnitude higher reaction rates (Refs 19–25). In 2020, the experiment carried out by Giuffrida et al. (Ref. 23) measured as much as 10^{11} α particles emitted during a single laser pulse at 10^{16} W/cm^2. Composite targets were used in some of these experiments, forming a proton-enriched plasma, in which protons and boron ions could react directly. However, so far, there is no report that a solid hydrogen-enriched boron target can also increase the fusion reaction yield.

Given the lack of further investigations in the low energy regime and the promising results obtained from laser-driven hydrogen-enriched plasma, we conducted an experiment on p-^{11}B fusion using a proton beam in the energy range of 120–260 keV from the accelerator at the Institute of Modern Physics (IMP, Lanzhou). Solid state targets of boron with natural isotope composition and hydrogen–boron (HB)-mixed were used. Notably, we observed the first experimental evidence of an apparent increase in p-^{11}B reactions at the HB target.

2. Experiment set-up

The experiment was carried out at the 320 kV high-voltage platform at IMP, Chinese Academy of Sciences. The proton beam, produced by an electron cyclotron resonance ion source and accelerated to 120–260 keV, was transported to the target chamber after a series of beam optical components. At the target, the beam current was around 1 μA and the beam diameter was about 5 mm. A transmitting Faraday cup (tFC) equipped with a 3 mm diaphragm in front of the target was monitoring the beam current *in-situ*, while a regular Faraday cup (FC) was applied after the target to calibrate the real beam current. The schematic diagram of the experiment set-up is shown in Fig. 2.

The detectors and the preamplifiers used to measure the α particles produced from the p-^{11}B reaction were developed in-house. The ion detector consists of 2 sets of 15-strips (10 mm × 2mm×150μm for each) of positive-intrinsic-negative (PIN) diodes (Ref. 26). To protect the PIN from scattered protons, they were covered by a Mylar film of 2 micron thickness and an additional 100 nm Al layer. These strips are arranged symmetrically on both sides of the beam at $\theta_{lab} = 100.5°$, with a total coverage area of approximately 0.3 sr. The pre-amplifiers were installed inside the target chamber where the vacuum remained at 10^{-7}mbar. The recorded signals from the PIN detectors were transmitted to the main amplifier (MSCF-16 Mesytec) and the data acquisition system through multi-pin coaxial cables and the feedthroughs. A N405 – Triple 4-Fold Logic Unit and a GG8020 Octal Gate and Delay Generator were used as the logic and gate control unit. A fast 32-channel Versa Module Eurocard peak sensing analog-to-digital converter converted the logic signals to the digital ones. Finally, we developed a data acquisition program based on the ROOT framework to record the data and to display the spectrum. All of the detectors and data acquisition system were pre-calibrated with a standard $Pu^{239} + Am^{241} + Cm^{244}$ α source (Refs 27–29), as shown in Fig. 3. The fit contains three Gaussian signal peaks and one continuum background. The total fitted result agrees with the calibration data quite well. The calibration introduces an uncertainty of approximately ±5%, which varies across different channels.

Figure 4 displays the targets used in our experiments and the typical characterization results. We used three different targets: a natural boron target and two HB targets, all with a size of 20 × 10 mm^2 and provided by the material technology group at ENN Energy Research Institute, China. The natural boron target was a block of 5 mm thickness with a density of 1.4 g/cm^3. The HB targets were manufactured by the plasma-enhanced chemical vapour deposition which deposited HB films on boron substrates. The HB-mixed layer on the targets is 1.5–2 μm thick and has a density of 1.3–1.5 g/cm^3, with a hydrogen atom concentration of about 25%. We determined the target characteristics using the weighing method, scanning electron microscope, elastic recoil and Rutherford backscattering diagnostics. The two HB targets yielded consistent experimental results in our study. To clarify our experimental conclusions and avoid redundancy, we only present the results from one of the HB targets in the following analysis, which we compare with the boron target.

3. Results

From $E_{lab} = 120$ to 260 keV, we performed measurements at 21 different proton beam energies with increments of 2 keV near the resonance energy of $E_{lab} = 162$ keV and big steps of 20 keV around 120 keV and 260 keV respectively. Figure 5 shows a comparison of the α particle energy spectra produced by the p-^{11}B nuclear reaction when 164 keV protons impinge the boron target and HB target. In both the boron target and the HB target, the spectrum clearly shows the α_0 and the α_1 emission, corresponding to the two different reaction pathways depicted in Fig. 1. The spectrum has been cut off at about 1.4 MeV. Considering the fact that the irradiation time per spectrum, and target densities are almost the same. It is obvious that for the HB target the p-^{11}B reaction yield is higher than in pure boron case. The curves also show that the factor of yield increase does not dependent on α energy (see lower part of Fig. 5), which indicates that all ^{12}C* decay channels are enhanced.

https://doi.org/10.1017/lpb.2024.2 Published online by Cambridge University Press

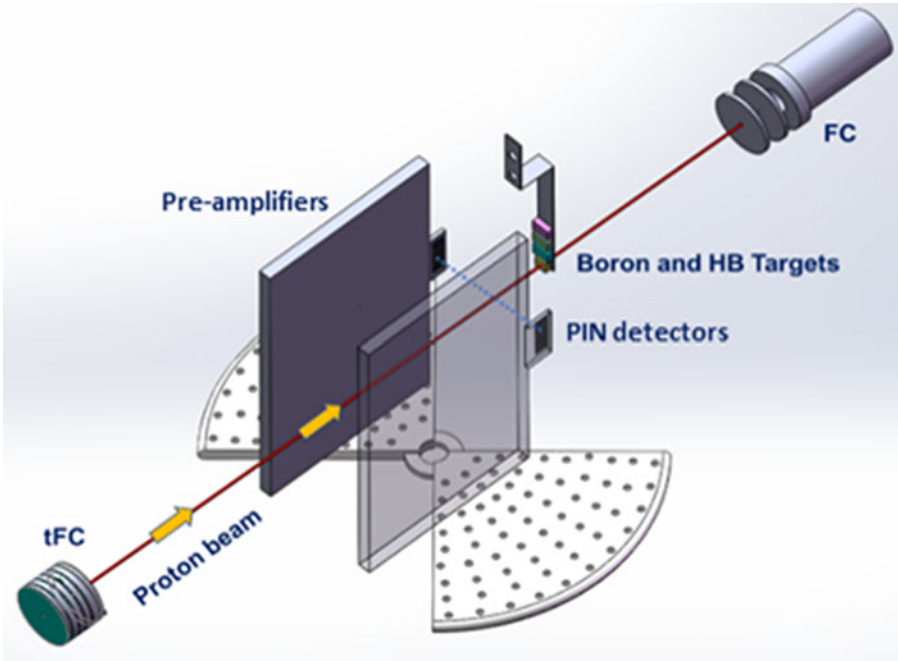

Figure 2. Schematically shows the experimental set-up at IMP. From left to right are: tFC, pre-amplifiers and detectors (parallelly placed), targets and the FC, respectively.

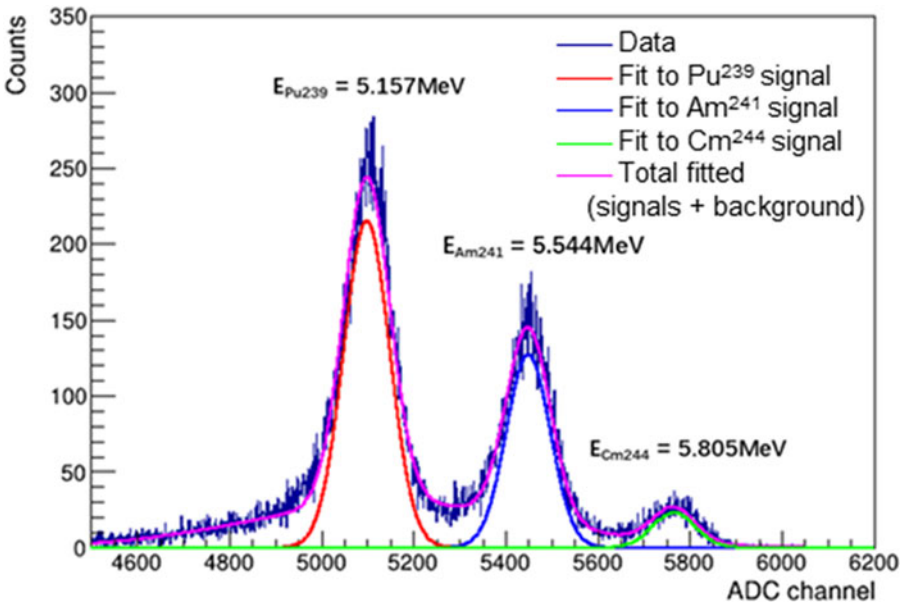

Figure 3. Energy calibration for source of $Pu^{239} + Am^{241} + Cm^{244}$, the three signals are fitted as Gaussians with backgrounds distributed continuously.

An appropriate comparison of the reaction rates from different targets requires normalization to the incident proton numbers (N_p) and the number density of boron atoms (N_b). When counting the yield of α particles (N_α), a correction based on the SRIM database (Ref. 30) has been taken into account. This correction accounts for the significant energy loss experienced by α particles as they penetrate through the targets. Spraker et al. (Ref. 31) derived the results in terms of counts/luminosity (X), in order to avoid figuring out all three emitted α particles from the spectrum. In thick targets, the proton incident depth is regarded as the target thickness, thus X is referred to as $\bar{X}$, the average differential cross section in intensity of α productions. It is calculated as:

$$\bar{X} = \frac{N_\alpha}{N_b N_p d\Omega} \ (\mathrm{cm}^2/\mathrm{sr}), \tag{2}$$

in which $d\Omega$ is the solid angle of each strip. Systematic uncertainties are dominating the experimental uncertainty. They are mainly due to beam fluctuations (less than $\pm 14\%$, varying in different shots) and the energy calibration (less than $\pm 10\%$, varying in different shots and detection channels). The statistical errors contribute only little to the total uncertainty, since they are on the order of 0.5%. The comparison between different targets is shown in Fig. 6.

In theory, the prediction of Nevins' analytic approximation (Ref. 14) can also be applied to derive to $\bar{X}$:

$$\bar{X} = \frac{R_{\mathrm{eff}}}{4\pi} \int_0^{E_p} \sigma(E) \times \left(\frac{\mathrm{d}E}{\mathrm{d}x}\right)^{-1} \mathrm{d}E, \tag{3}$$

https://doi.org/10.1017/lpb.2024.2 Published online by Cambridge University Press

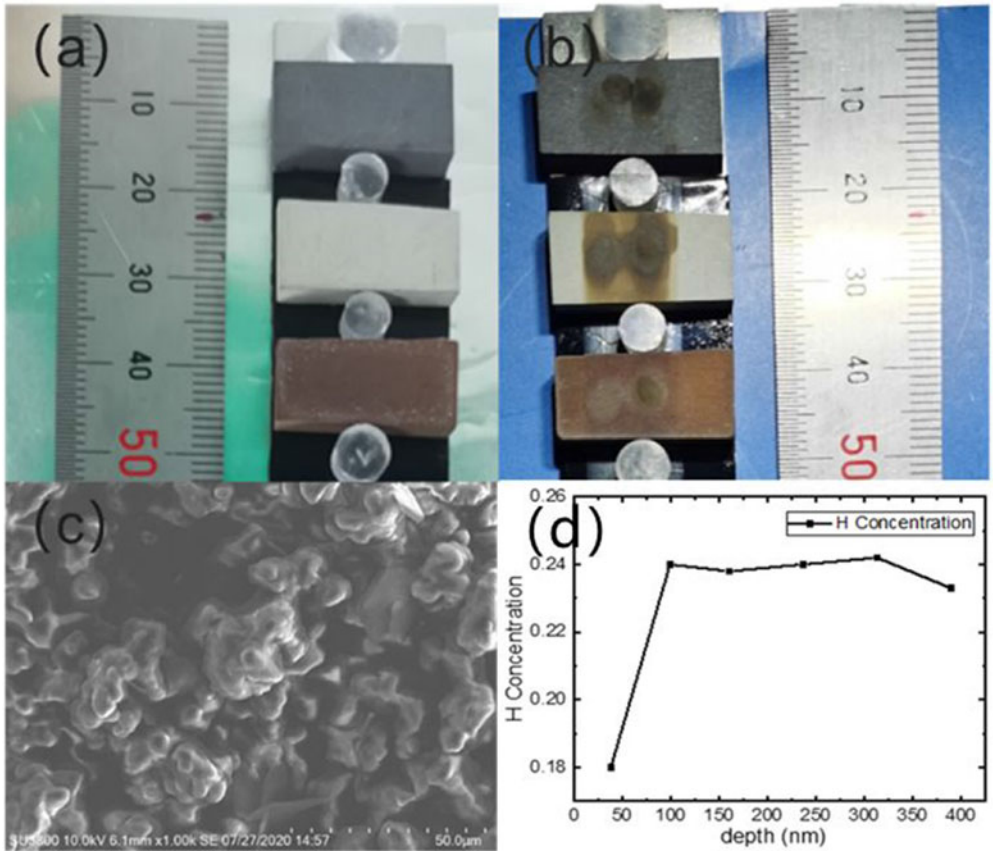

Figure 4. Targets before (a) and after (b) the experiment, boron, two HB targets are listed from top to the bottom. The characteristics for HB target by scanning electron microscope (SEM) and elastic recoil detection (ERD) are shown in (c) and (d).

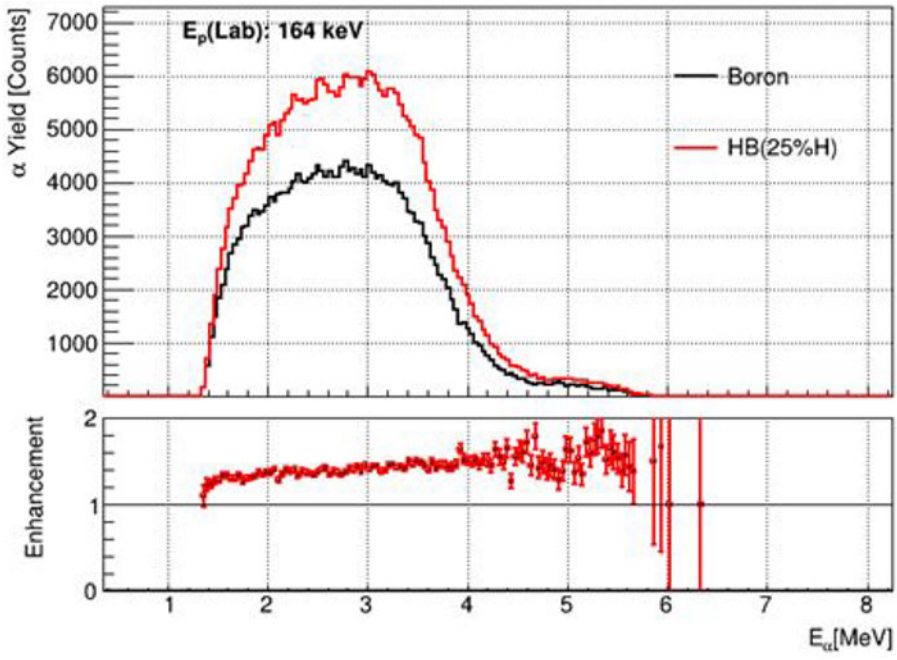

Figure 5. A typical α spectrum at $E_{lab} = 164$ keV, comparing the boron (black) and HB (red) targets.

in which R_{eff} is the rate of detection efficiency estimated by the α source calibration, at $\pm 34.4\%$. The stopping power $(\mathrm{d}E/\mathrm{d}X)$ is estimated by SRIM (Ref. 30), whose systematic errors were evaluated by Paul (Ref. 32), to have an impact of $\pm 0.5\%$ on the final results, for both proton and α particles. At last, a systematic uncertainty on the detector location and size is evaluated as $+24.2\% / -21.6\%$, and the theoretical error on the approximation is derived as $\pm 7.81\%$. All detector and theory uncertainties are considered

https://doi.org/10.1017/lpb.2024.2 Published online by Cambridge University Press

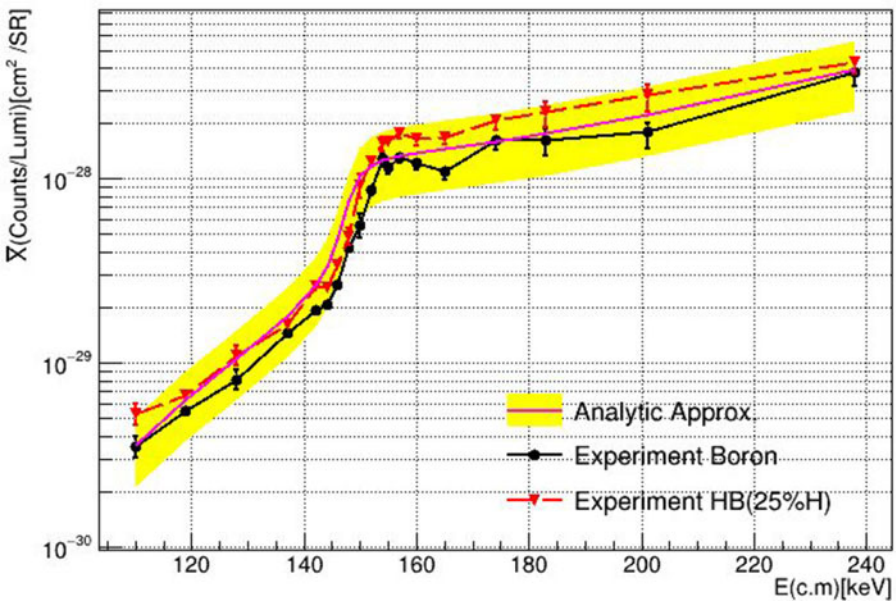

Figure 6. Comparison of $\bar{X}$ for different targets and the analytic approximation by Nevins et al. (Ref. 14) among centre-of-mass energy between 110 and 240 keV. The experimental results in HB target are shown as red curves with dots, while the boron target result is displayed as a black solid curve with dots. Error bars on each point represent the sum of experimental and statistical uncertainties. The prediction has been given in magenta curves with a yellow error band, which includes the uncertainties of approximation and detector efficiency variations.

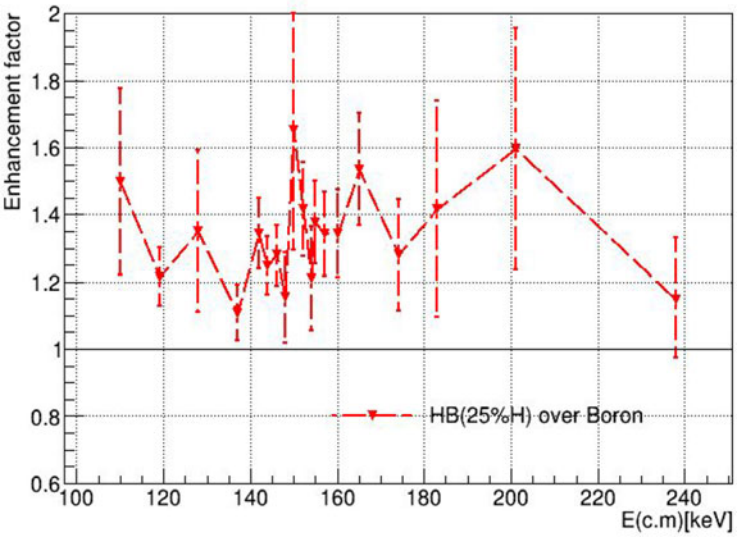

Figure 7. The enhancement factor of HB target to pure boron target among centre-of-mass energy between 110 and 240 keV. The red solid line with points represents the enhancements of HB target with error. The line shows a scale of 1.

only when we compare to the analytic approximation, shown as the yellow band in Fig. 6. The experiment and prediction are in good agreement within 1σ variation.

Figure 7 shows the enhancement factor of production yield in HB target over pure boron target. An average of 30% excess is observed for HB target among the energy points between $E_{c.m.} =$ 110 and 240 keV. The enhancement factor is around 1.3 and exceeds the 1σ error band at most energy points. No clear trend was found for the enhancement factor as a function of energy, which is against a potential explanation of screening effect (Refs 33–35).

4. Discussion

To the best of our knowledge, this experiment is the first to demonstrate that HB targets can generate a higher intensity of α particles in the energy range of 120–260 keV for protons. By introducing hydrogen atoms into the solid boron target, we observed a reaction yield excess similar to what has been observed in high-profile laser-driven p-^{11}B reaction experiments (Refs 20–25), albeit under very different experimental conditions with respect to proton beam intensity, proton energy and here the target is not in a plasma state. The mechanism behind this observation has yet to be determined.

Hora and Eliezer et al. (Refs 36, 37) have put forward a potential avalanche process that suggests α particles in plasma can generate protons with energies around the largest resonance peak (675 keV) via two consecutive collisions with high momentum transfer, leading to an increase in the yield of the p-^{11}B fusion reaction. However, in dense solid targets and in the proton energy range considered here electronic collisions with bound target electrons dominate the energy loss process. The range of α particles is therefore limited to just a few microns, making the likelihood of two consecutive hard collisions extremely low (Refs 38, 39), and thus we expect this to have a negligible effect on the yield. Another potential explanation

https://doi.org/10.1017/lpb.2024.2 Published online by Cambridge University Press

of the experimental observation also takes into account the large momentum transfer between α particles and protons, which suggests that protons gaining energy exceeding 1 MeV may be mistakenly identified as α particles by the detector. However, the lower part of Fig. 5 shows a uniform enhancement with increasing α energy, which is inconsistent with the expectation of alpha–proton (α-p) scattering. Also, our calculation indicates that the contribution is negligible, limited by the elastic scattering cross-section (Refs 38, 39).

Ren et al. (Ref. 40) have recently proposed an alternative theory to explain the gain in laser-driven p-^{11}B reactions, suggesting that the localized electric field induced by an intense beam alters the energy loss of protons in plasma, thereby enhancing the reaction rate. Also, this theory does not apply to the beam intensity or target type used in our experiment and cannot account for the difference in p-^{11}B reaction rates between boron and HB targets. We also do not consider the screening effect (Refs 33–35) as the driving mechanism behind the increased yield, which suggests a 10% deviation compared to the bare system at 100 keV (Ref. 33). This effect cannot explain the differences between solid HB and pure boron targets, and we did not observe any trend in the gain coefficient with respect to changes in energy (see Fig. 7).

The most likely explanation for the increased yield in our experiment is the contribution of protons affected by elastic upscattering of α particles to the secondary reaction, which could be higher than expected. Previous studies have focused on elastic scatterings involving high momentum transfer (Refs 36, 37). It is worth noting that the p-^{11}B reaction has a resonance peak at as low as162 keV, and as a result, the secondary reaction caused by α-p small-angle Rutherford scattering cannot be ignored. The differential scattering cross section could be as high as 35.4 b/sr for a 4 MeV α particle producing a 200 keV proton, according to the Rutherford law (Refs 41, 42), and drives secondary and even multiple reactions. Currently, we are conducting comprehensive theoretical and simulation work to support this explanation. Measuring the Rutherford cross section of α-p at small scattering angles in experiments can be challenging, but the results of this experiment have the potential to provide corrections to improve the theoretical model.

According to calculations by Putvinski et al. (Ref. 17), using cross section data by Sikora et al. (Ref. 43) instead of Nevins et al. (Ref. 14) (which are approximately 20% larger at $E_{\mathrm{c.m.}} < 1$ MeV) could allow the fusion power to overcome the radiation loss due to Bremsstrahlung at T_i300 keV. An enhancement of 30% in reaction yield, as presented in our work in the low energy region, can also contribute to achieving this breakthrough and further lower the optimum T_i. A recent study by Xie et al. (Ref. 44) shows that an increase of 20% in reactivity could significantly lower the Lawson criteria (Refs 45, 46). Therefore, further exploration of p-^{11}B reactions in low energy regime is crucial for thermonuclear fusion research. With a deeper understanding, the feasibility of p-^{11}B fusion as a future energy source is gradually increasing.

5. Conclusion

In this study, we report on measurements of the α particle yields in p-^{11}B reactions from pure boron and hydrogen-doped (HB) targets for the proton energy range $E_{\mathrm{lab}} = 120$ to 260 keV. We find good agreement with Nevins' model (Ref. 14). Notably, we observe a 30% increase in α particle yield for the HB target, which is significant even considering the 1σ error band. This is the first time that experimental evidence has been reported for an increase in reaction yield from a hydrogen-doped-boron target. Based on our observations, we believe the most likely theoretical explanation is that α particles undergo small-angle elastic scattering with hydrogen atoms in the HB target, producing a significant amount of protons above 100 keV that participate in secondary reactions. We are currently conducting comprehensive simulation calculations based on theoretical models and plan to further investigate the influence of different hydrogen atom concentrations in the HB target on the experimental results. We call for more independent experiments and studies on this topic. The low energy regime is not well explored, and further studies may yield more clues about the possibility of p-^{11}B fusion in general and, especially in the keV energy regime, for future fusion energy applications.

Acknowledgements. The authors sincerely acknowledge the technical support from the group of 320 kV HCI platform at IMP. We would like to appreciate Ong Hooi Jin and Jianguo Wang's guidance in building the data acquisition system and also thanks to Yang Li and Jianhua Feng for the help during the experiment.

References

1. **Ning X, Liang T, Wu D, Liu S, Liu Y, Hu T, Sheng Z, Ren J, Jiang B, Zhao Y, Hoffmann DHH and He XT** (2022) Laser-driven proton-boron fusions: Influences of the boron state. *Laser and Particle Beams* **2022**, 9868807.
2. **Zylstra AB, Hurricane OA, Callahan DA, Kritcher AL, Ralph JE, Robey HF, Ross JS, Young CV, Baker KL, Casey DT, Döppner T, Divol L, Hohenberger M, Le Pape S, Pak A, Patel PK, Tommasini R, Ali SJ, Amendt PA, Atherton LJ, Bachmann B, Bailey D, Benedetti LR, Berzak Hopkins L, Betti R, Bhandarkar SD, Biener J, Bionta RM, Birge NW, Bond EJ, Bradley DK, Braun T, Briggs TM, Bruhn MW, Celliers PM, Chang B, Chapman T, Chen H, Choate C, Christopherson AR, Clark DS, Crippen JW, Dewald EL, Dittrich TR, Edwards MJ, Farmer WA, Field JE, Fittinghoff D, Frenje J, Gaffney J, Gatu Johnson M, Glenzer SH, Grim GP, Haan S, Hahn KD, Hall GN, Hammel BA, Harte J, Hartouni E, Heebner JE, Hernandez VJ, Herrmann H, Herrmann MC, Hinkel DE, Ho DD, Holder JP, Hsing WW, Huang H, Humbird KD, Izumi N, Jarrott LC, Jeet J, Jones O, Kerbel GD, Kerr SM, Khan SF, Kilkenny J, Kim Y, Geppert Kleinrath H, Geppert Kleinrath V, Kong C, Koning JM, Kroll JJ, Kruse MKG, Kustowski B, Landen OL, Langer S, Larson D, Lemos NC, Lindl JD, Ma T, MacDonald MJ, MacGowan BJ, Mackinnon AJ, MacLaren SA, MacPhee AG, Marinak MM, Mariscal DA, Marley EV, Masse L, Meaney K, Meezan NB, Michel PA, Millot M, Milovich JL, Moody JD, Moore AS, Morton JW, Murphy T, Newman K, Di Nicola J-MG, Nikroo A, Nora R, Patel MV, Pelz LJ, Peterson JL, Ping Y, Pollock BB, Ratledge M, Rice NG, Rinderknecht H, Rosen M, Rubery MS, Salmonson JD, Sater J, Schiaffino S, Schlossberg DJ, Schneider MB, Schroeder CR, Scott HA, Sepke SM, Sequoia K, Sherlock MW, Shin S, Smalyuk VA, Spears BK, Springer PT, Stadermann M, Stoupin S, Strozzi DJ, Suter LJ, Thomas CA, Town RPJ, Tubman ER, Trosseille C, Volegov PL, Weber CR, Widmann K, Wild C, Wilde CH, Van Wonterghem BM, Woods DT, Woodworth BN, Yamaguchi M, Yang ST and Zimmerman GB** (2022) Burning plasma achieved in inertial fusion. *Nature* **601**, 542–548.
3. **Clery D** (2022) European fusion reactor sets record for sustained energy. *Science* **375**, 600.
4. **Li J, Guo HY, Wan BN, Gong XZ, Liang YF, Xu GS, Gan KF, Hu JS, Wang HQ, Wang L, Zeng L, Zhao YP, Denner P, Jackson GL, Loarte A, Maingi R, Menard JE, Rack M and Zou XL** (2013) A long-pulse high-confinement plasma regime in the Experimental Advanced Superconducting Tokamak. *Nature Physics* **9**, 817–821.
5. **Collaboration IDICF, Abu-Shawareb H, Acree R, Adams P, Adams J, Addis B, Aden R, Adrian P, Afeyan BB, Aggleton M, Aghaian L, Aguirre A, Aikens D, Akre J, Albert F, Albrecht M, Albright BJ, Albritton J, Alcala J, Alday C, Alessi DA, Alexander N, Alfonso J,**

https://doi.org/10.1017/lpb.2024.2 Published online by Cambridge University Press

Alfonso N, Alger E, Ali SJ, Ali ZA, Alley WE, Amala P, Amendt PA, Amick P, Ammula S, Amorin C, Ampleford DJ, Anderson RW, Anklam T, Antipa N, Appelbe B, Aracne-Ruddle C, Araya E, Arend M, Arnold P, Arnold T, Asay J, Atherton LJ, Atkinson D, Atkinson R, Auerbach JM, Austin B, Auyang L, Awwal AS, Ayers J, Ayers S, Ayers T, Azevedo S, Bachmann B, Back CA, Bae J, Bailey DS, Bailey J, Baisden T, Baker KL, Baldis H, Barber D, Barberis M, Barker D, Barnes A, Barnes CW, Barrios MA, Barty C, Bass I, Batha SH, Baxamusa SH, Bazan G, Beagle JK, Beale R, Beck BR, Beck JB, Bedzyk M, Beeler RG, Behrendt W, Belk L, Bell P, Belyaev M, Benage JF, Bennett G, Benedetti LR, Benedict LX, Berger R, Bernat T, Bernstein L A, Berry B, Bertolini L, Besenbruch G, Betcher J, Bettenhausen R, Betti R, et al (2022) Lawson criterion for ignition exceeded in an inertial fusion experiment. *Physical Review Letters* **129**, 75001.

6. **Hoffmann D, Richter A, Schrieder G and Seegebarth K** (1983) Cross section for the reaction C-12(e,p)B-11; and its relevance to the formation of B-11 in active galaxies. *The Astrophysical Journal* **271**, 398–403.
7. **Calarco JR, Arruda-Neto J, Griffioen KA, Hanna SS, Hoffmann DHH, Neyer B, Rand RE, Wienhard K and Yearian MR** (1984) Observation of monopole strength in the 12C (e, e′ p_0^{11}B reaction. *Physics Letters B* **146**, 179–182.
8. **Cai J, Xie H, Li Y, Tuszewski M, Zhou H and Chen P** (2022) A study of the requirements of p-^{11}B fusion reactor by tokamak system code. *Fusion Science and Technology* **78**, 149–163.
9. **Yoon D-K, Jung J-Y and Suh TS** (2014) Application of proton boron fusion reaction to radiation therapy: A Monte Carlo simulation study. *Applied Physics Letters* **105**, 223507.
10. **Cirrone GAP, Manti L, Margarone D, Petringa G, Giuffrida L, Minopoli A, Picciotto A, Russo G, Cammarata F and Pisciotta P** (2018) First experimental proof of Proton Boron Capture Therapy (PBCT) to enhance protontherapy effectiveness. *Scientific Reports* **8**, 1–15.
11. **Giuffrida L, Margarone D, Cirrone GAP, Picciotto A, Cuttone G and Korn G** (2016) Prompt gamma ray diagnostics and enhanced hadron-therapy using neutron-free nuclear reactions. *AIP Advances* **6**, 105204.
12. **Oliphant MLE and Rutherford E** (1933) Experiments on the transmutation of elements by protons. *Proceedings of the Royal Society of London: Series A, Containing Papers of a Mathematical and Physical Character* **141**, 259–281.
13. **Becker HW, Rolfs C and Trautvetter HP** (1987) Low-energy cross sections for ^{11}B (p, 3α). *Zeitschrift Für Physik A Atomic Nuclei* **327**, 341–355.
14. **Nevins WM and Swain R** (2000) The thermonuclear fusion rate coefficient for p-^{11}B reactions. *Nuclear Fusion* **40**, 865–872.
15. **Munch M, Kirsebom OS, Swartz JA and Fynbo HOU** (2020) Resolving the 11B (p, α) cross-section discrepancies between 0.5 and 3.5 MeV. *European Physical Journal A: Hadrons and Nuclei* **56**, 17.
16. **Otuka N, Dupont E, Semkova V, Pritychenko B, Blokhin AI, Aikawa M, Babykina S, Bossant M, Chen G and Dunaeva S** (2014) Towards a more complete and accurate experimental nuclear reaction data library (EXFOR): International collaboration between nuclear reaction data centres (NRDC). *Nuclear Data Sheets* **120**, 272–276.
17. **Putvinski SV, Ryutov DD and Yushmanov PN** (2019) Fusion reactivity of the pB^{11} plasma revisited. *Nuclear Fusion* **59**, 076018.
18. **Magee RM, Ogawa K, Tajima T, Allfrey I, Gota H, McCarroll P, Ohdachi S, Isobe M, Kamio S, Klumper V, Nuga H, Shoji M, Ziaei S, Binderbauer MW and Osakabe M** (2023) First measurements of p^{11}B fusion in a magnetically confined plasma. *Nature Communications* **14**, 955.
19. **Belyaev VS, Matafonov AP, Vinogradov VI, Krainov VP, Lisitsa VS, Roussetski AS, Ignatyev GN and Andrianov VP** (2005) Observation of neutronless fusion reactions in picosecond laser plasmas. *Physical Review E: Statistical, Nonlinear, and Soft Matter Physics* **72**, 9–13.
20. **Labaune C, Baccou C, Depierreux S, Goyon C, Loisel G, Yahia V and Rafelski J** (2013) Fusion reactions initiated by laser-accelerated particle beams in a laser-produced plasma. *Nature Communications* **4**, 1–6.
21. **Picciotto A, Margarone D, Velyhan A, Bellutti P, Krasa J, Szydlowsky A, Bertuccio G, Shi Y, Mangione A and Prokupek J** (2014) Boron-proton nuclear-fusion enhancement induced in boron-doped silicon targets by low-contrast pulsed laser. *Physical Review X* **4**, 31030.
22. **Margarone D, Picciotto A, Velyhan A, Krasa J, Kucharik M, Morrissey M, Mangione A, Szydlowsky A, Malinowska A, Bertuccio G, Shi Y, Crivellari M, Ullschmied J, Bellutti P and Korn G** (2015) Advanced scheme for high-yield laser driven proton-boron fusion reaction. *High Power Lasers for Fusion Research III* **9345**, 93450F.
23. **Giuffrida L, Belloni F, Margarone D, Petringa G, Milluzzo G, Scuderi V, Velyhan A, Rosinski M, Picciotto A, Kucharik M, Dostal J, Dudzak R, Krasa J, Istokskaia V, Catalano R, Tudisco S, Verona C, Jungwirth K, Bellutti P, Korn G and Cirrone GAP** (2020) High-current stream of energetic α particles from laser-driven proton-boron fusion. *Physical Review E* **101**, 1–13.
24. **Margarone D, Bonvalet J, Giuffrida L, Morace A, Kantarelou V, Tosca M, Raffestin D, Nicolai P, Picciotto A, Abe Y, Arikawa Y, Fujioka S, Fukuda Y, Kuramitsu Y, Habara H and Batani D** (2022) In-target proton–boron nuclear fusion using a PW-class laser. *Applied Sciences* **12**, 1444.
25. **Istokskaia V, Tosca M, Giuffrida L, Psikal J, Grepl F, Kantarelou V, Stancek S, Di Siena S, Hadjikyriacou A, McIlvenny A, Levy Y, Huynh J, Cimrman M, Pleskunov P, Nikitin D, Choukourov A, Belloni F, Picciotto A, Kar S, Borghesi M, Lucianetti A, Mocek T and Margarone D** (2023) A multi-MeV alpha particle source via proton-boron fusion driven by a 10-GW tabletop laser. *Communications Physics* **6**, 27.
26. **Chen C-H, Z-k L, Wang X-H, R-h L, Fang F, Wang Z-S and Li H-X** (2023) Development of high performance PIN-silicon detector and its application in radioactive beam physical experiment. *Acta Physica Sinica* **72**, 122902–122909.
27. **Adams JP and Carboneau ML** (1999) *National Low-Level Waste Management Program Radionuclide Report Series, Volume 17: Plutonium-239*. Idaho Falls, ID: Idaho National Lab. (INL).
28. **Winberg MR and Garcia RS** (1995) *National Low-Level Waste Management Program Radionuclide Report Series, Volume 14: Americium-241* (EG and G Idaho).
29. **Hummel JP** (1956) *Alpha-Decay Studies in the Heavy-Element Region (Thesis)* (United States).
30. **Ziegler JF, Ziegler MD and Biersack JP** (2010) SRIM – The stopping and range of ions in matter. *Nuclear Instruments and Methods in Physics Research Section B: Beam Interactions with Materials and Atoms* **268**, 1818–1823.
31. **Spraker MC, Ahmed MW, Blackston MA, Brown N, France RH, Henshaw SS, Perdue BA, Prior RM, Seo PN, Stave S and Weller HR** (2012) The 11B(p,α) 8Be $\rightarrow \alpha + \alpha$ and the 11B(α,α) 11B reactions at energies below 5.4 MeV. *Journal of Fusion Energy* **31**, 357–367.
32. **Paul H and Schinner A** (2006) Statistical analysis of stopping data for protons and alphas in compounds. *Nuclear Instruments and Methods in Physics Research Section B: Beam Interactions with Materials and Atoms* **249**, 1–5.
33. **Assenbaum HJ, Langanke K and Rolfs C** (1987) Effects of electron screening on low-energy fusion cross sections. *Zeitschrift Für Physik A Atomic Nuclei* **327**, 461–468.
34. **Kimura S and Bonasera A** (2005) Influence of the electronic chaotic motion on the fusion dynamics at astrophysical energies. *Nuclear Physics A* **759**, 229–244.
35. **Bencze G** (1989) Electron screening effects in low-energy fusion reactions. *Nuclear Physics A* **492**, 459–472.
36. **Hora H, Korn G, Giuffrida L, Margarone D, Picciotto A, Krasa J, Jungwirth K, Ullschmied J, Lalousis P, Eliezer S, Miley GH, Moustaizis S and Mourou G** (2015) Fusion energy using avalanche increased boron reactions for block-ignition by ultrahigh power picosecond laser pulses. *Laser and Particle Beams* **33**, 607–619.
37. **Eliezer S, Hora H, Korn G, Nissim N and Martinez Val JM** (2016) Avalanche proton-boron fusion based on elastic nuclear collisions. *Physics of Plasmas* **23**, 050704.
38. **Wang Y, Chen J and Huang F** (1986) The calculation of the differential cross sections for recoil protons in ^{4}He-p scattering. *Nuclear Instruments and Methods in Physics Research Section B: Beam Interactions with Materials and Atoms* **17**, 11–14.

https://doi.org/10.1017/lpb.2024.2 Published online by Cambridge University Press

39. **Bogdanović Radović I and Benka O** (2001) Determination of H recoil cross-sections for He ions incident at 2.5–4.5 MeV and recoil angles from 30° to 60°. *Nuclear Instruments and Methods in Physics Research Section B: Beam Interactions with Materials and Atoms* **174**, 25–32.
40. **Ren J, Deng Z, Qi W, Chen B, Ma B, Wang X, Yin S, Feng J, Liu W, Xu Z, Hoffmann DHH, Wang S, Fan Q, Cui B, He S, Cao Z, Zhao Z, Cao L, Gu Y, Zhu S, Cheng R, Zhou X, Xiao G, Zhao H, Zhang Y, Zhang Z, Li Y, Wu D, Zhou W and Zhao Y** (2020) Observation of a high degree of stopping for laser-accelerated intense proton beams in dense ionized matter. *Nature Communications* **11**, 1–7.
41. **Rutherford E** (1911) LXXIX. The scattering of α and β particles by matter and the structure of the atom. *The London, Edinburgh, and Dublin Philosophical Magazine and Journal of Science* **21**, 669–688.
42. **Kamal AA** (2010) Nuclear Physics – I BT – 1000 Solved Problems in Modern Physics ed A A Kamal. Berlin, Heidelberg: Springer Berlin Heidelberg,369–425
43. **Sikora MH and Weller HR** (2016) A new evaluation of the 11 B(p, α) αα reaction rates. *Journal of Fusion Energy* **35**, 538–543.
44. **Xie H, Tan M, Luo D, Li Z and Liu B** (2023) Fusion reactivities with drift bi-Maxwellian ion velocity distributions. *Plasma Physics and Controlled Fusion* **65**, 55019.
45. **Lawson JD** (1957) Some criteria for a power producing thermonuclear reactor. *Proceedings of the Physical Society. Section B* **70**, 6.
46. **Wurzel SE and Hsu SC** (2022) Progress toward fusion energy breakeven and gain as measured against the Lawson criterion. *Physics of Plasmas* **29**, 62103.

https://doi.org/10.1017/lpb.2024.2 Published online by Cambridge University Press